Journal of Fluorine Chemistry 162 (2014) 1–8

Contents lists available at ScienceDirect

Journal of Fluorine Chemistry

journal homepage: www.elsevier.com/locate/fluor

Separation of metallic residues from the dissolution of a high-burnup BWR fuel using nitrogen trifluoride

Bruce K. McNamara *, Edgar C. Buck, Chuck Z. Soderquist, Frances N. Smith, Edward J. Mausolf, Randall D. Scheele

Energy and Environment Directorate, Nuclear Chemistry and Engineering Group, Pacific Northwest National Laboratory, Richland, WA 99352, United States

ARTICLE INFO

Article history:
Received 16 November 2013
Received in revised form 23 February 2014
Accepted 26 February 2014
Available online 23 March 2014

Keywords:
Noble metal phase
5-Metal phase
White inclusions
Nitrogen trifluoride
Fluoride volatility
Platinum metals

ABSTRACT

Nitrogen trifluoride (NF_3) was used to fluorinate the metallic residue from the dissolution of a high burnup, boiling water reactor fuel (~70 MWd/kgU). The washed residue included the noble-metal phase (containing ruthenium, rhodium, palladium, technetium, and molybdenum), smaller amounts of zirconium, selenium, tellurium, and silver, along with trace quantities of plutonium, uranium, cesium, cobalt, europium, and americium, likely as their oxides. Exposing the noble metal phase to 10% NF_3 in argon, between 400 and 550 °C, removed molybdenum and technetium near 400 °C as their volatile fluorides, and ruthenium near 500 °C as its volatile fluoride. The events were thermally and temporally distinct and the conditions specified provide a recipe to separate these transition metals from each other and from the nonvolatile residue. Depletion of the volatile fluorides resulted in substantial exothermicity. Thermal excursion behavior was recorded with the thermal gravimetric instrument operated in a non-adiabatic, isothermal mode; conditions that typically minimize heat release. Physical characterization of the noble-metal phase and its thermal behavior are consistent with high kinetic velocity reactions encouraged by the nanoparticulate phase or perhaps catalytic influences of the mixed platinum metals with nearly pure phase structure. Post-fluorination, only two products were present in the residual nonvolatile fraction. These were identified as a nano-crystalline, metallic palladium cubic phase and a hexagonal rhodium trifluoride (RhF_3) phase. The two phases were distinct as the sub-μm crystallites of metallic palladium were in contrast to the RhF_3 phase, which grew from the parent, nano-crystalline noble-metal phase during fluorination, to acicular crystals exceeding 20-μm in length.

1. Introduction

The use of fluoride volatility has long been considered a potential approach for separating commercial used nuclear fuel constituents, particularly uranium and plutonium [1–5]. We have been investigating the use of nitrogen trifluoride (NF_3) [6–8] as a fluorinating agent to recover desirable products from intractable matrices, including used nuclear fuel. The use of aggressive fluorinating reagents, such as molecular fluorine (F_2) and chlorine trifluoride (ClF_3), results in collective volatilization of a large number of constituents that are present in used fuel [5]. Proposed large-scale fluoride volatility separations [1–5] of used fuel thus require several additional steps to recover the valuable components from the volatile product stream. The lower reactivity of NF_3, relative to that of F_2 and ClF_3, alters the individual fluoride product distributions and onset temperatures for volatilization of constituents in the used fuel. As a consequence, sequential separations of smaller groupings of the volatile fuel constituents can be realized, especially if the heats of reaction are regulated [6–8], and the requirements for further separations, reduced. In this article, we use this ability of NF_3 to sequentially separate a particularly unreactive but valuable alloy found in used nuclear fuel.

Irradiated uranium dioxide (UO_2) or mixed uranium and plutonium oxide (MOX) nuclear fuel is generally described as a complex mixture of solid solutions of metal oxides, oxide particles that are at least partially insoluble in the primary fuel matrix, and a metallic phase composed of technetium (Tc), molybdenum (Mo), and the platinum metals: ruthenium (Ru), rhodium (Rh), and palladium (Pd) [9,10]. The metal phase is cited in the literature as the "white inclusions" [11], the "epsilon phase (ε)" [12], the "5-metal

* Corresponding author. Tel.: +1 5093755678.
E-mail address: bruce.mcnamara@pnnl.gov (B.K. McNamara).

http://dx.doi.org/10.1016/j.jfluchem.2014.02.010
0022-1139/

phase" [12], or the "noble-metal phase" [13]. The latter term will be used here in reference to the unreactive nature of the platinum metals contained in this phase.

The structure of the noble-metal phase is often cited as hexagonal close packed (hcp) [10,14,15], but earlier efforts [10,16] and ongoing work in our laboratory indicates variation in structure from single hcp and body centered cubic (bcc) phases, to biphasic and triphasic hcp, bcc, and face-centered cubic (fcc) combinations. The phase has been shown by several authors to exist as finely dispersed particles throughout irradiated fuel [10,12]. The phase does not dissolve in boiling nitric acid and historically has been discarded, along with other insoluble material, as the residue from used fuel dissolution. A number of characterizations of the noble-metal phase have been discussed in the literature and remain of interest to issues concerning used nuclear fuel disposition. First, the narrow (1–5 nm) size distribution of the noble-metal phase residues collected from dissolution of several common fuel types [15,17,18] could be responsible for fires during storage of used fuel hulls at industrial sites, and for the rapid release of radiotoxic ruthenium during reprocessing of fuel [19] and during nuclear accident scenarios [20]. Second, the noble-metal phase is comprised of catalytic metals and if the phase is itself catalytic, its reactivity with hydrogen [21], oxygen, and biogenic sulfur, could have implications for its long term storage in proposed nuclear fuel emplacements [22]. Finally, the phase is a recoverable source of the platinum metals: Ru, Rh, Pd [23]. Recent reviews that discuss aqueous and pyrochemical methods of platinum metals recovery from used nuclear fuel, do not address fluoride volatility [24,25].

The used fuel used in this study is representative of nuclear fuels from light water, boiling water and pressure water reactors in use in the US, India, China, and Japan. The high surface area of the noble-metal phase described here and in other studies [14,15] should be common to used fuels from these reactor types. The fine grained nature of the particles suggest that melting and aggregation to larger particles during irradiation, as has been proposed for used fuels from higher temperature nuclear reactor designs did not occur. Preparations of surrogates of the noble-metal phase have been reported to melt above 1500 °C [26]. These data [26] and those from dissolution studies [18,27] are consistent with a material that is quite refractory as well as chemically inert. Nevertheless, several studies indicated to us that inventory [5] concentrations of Mo, Tc, Ru, and perhaps Rh are expected to be released from used nuclear fuel when it is reacted with fluorine gas (F_2) [1]. Consequently, it was of interest to investigate if NF_3 would react with the noble-metal phase and permit volatility separation of its constituents. The first fluoride volatility separation of this chemically inert alloy from used fuel is presented. The separation was accompanied by atypical exothermicity and the residual products of fluorination were novel in several ways. Microscopic characterization of the starting and end products are discussed to illuminate the underlying causes of enhanced reactivity of this unusual material.

2. Results

The noble-metal phase described here was obtained by dissolving commercial used nuclear fuel [28] from its cladding at room temperature, in a 1.5 M ammonium carbonate solution with 30% hydrogen peroxide as oxidant [17]. The dissolution was done using approximately 15 g of three different burn-up fuels and was repeated using boiling nitric acid for these fuels. The residues of the dissolutions were washed with 0.5 M nitric acid and water. Comparisons of the dissolution methods for such residues have been reported [18] and compared to examinations by others [12,15] that used nitric acid dissolution of the fuels. Here, the material was first characterized by scanning electron microscopy (SEM) coupled with energy dispersive X-ray spectroscopy (EDS) and transmission electron microscopy (TEM). The thermal behavior of the washed residue with 10% NF in argon (Ar) was then followed by thermogravimetry, and the post-fluorination residue was characterized by SEM/EDS and TEM. Supporting thermogravimetric (TG) characterizations of the reactions of NF_3 with a surrogate noble-metal phase [26], neat Ru and Rh metal powders and their oxides are also reported. Unpublished thermal and product characterization data for the reactions of NF_3 with neat nuclear fuel metal and oxide constituents are presented in Table S1 in the Supplementary Data Section.

2.1. Characterization of the noble phase

The SEM image and EDS spectrum of the insoluble residue are shown in Fig. 1. In this lower magnification view, the particles in the residue appear as μm and sub-μm in size, as was commonly cited in the early literature on these materials [10,16]. While the EDS analysis indicated a noble-metal phase; Mo, Tc, Rh, and Pd, with the commonly cited hcp composition [14,15], the residue also contained lesser concentrations of fission products: selenium (Se), tellurium (Te), zirconium (Zr), silver (Ag), iodide (I), uranium (U) and plutonium (Pu) and impurities silicon (Si), chromium (Cr), and

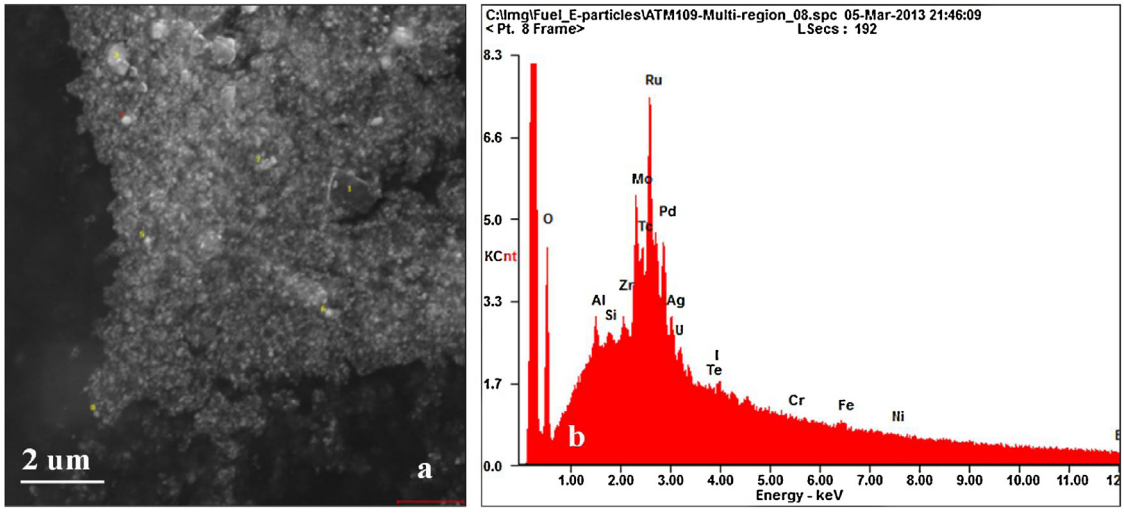

Fig. 1. SEM image and EDS spectrum of the residue from dissolving ATM-109 spent fuel in hydrogen peroxide/carbonate media. Note the apparent <1 μm size of the particles.

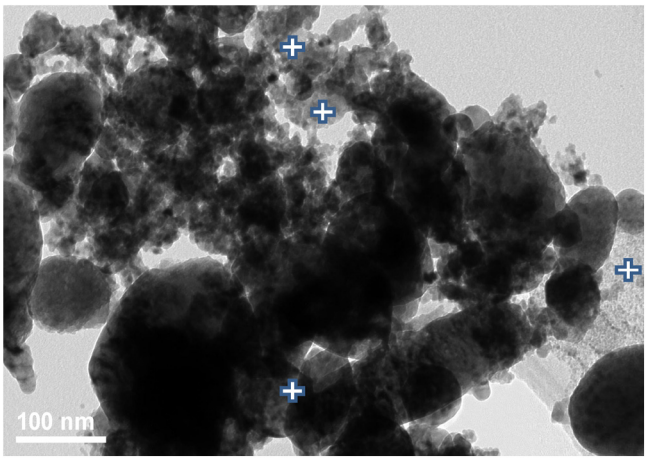

Fig. 2. High resolution TEM image of the noble-metal phase residue. In this view, the particle size is seen to be more realistically 1–5 nm. The highlighted areas indicate the very finely grained ruthenium rich component that appeared to help agglomerate the darker five-metal phase particles.

iron (Fe), likely from processing containers in the shielded facility used to mitigate the radioactive hazard. Trace amounts of cobalt, cesium, europium, and americium, were identified as present by their gamma spectra but were not detected by SEM or TEM. It should be noted that the composition of the residues used in the separation of the noble phase here were exceptionally low in the Pu and uranium and other elemental content relative to those that might be found in different fuel types or in lower or higher burnup fuels.

The high resolution TEM image in Fig. 2 shows that the larger particles in Fig. 1 were actually aggregates of 20–50 nm oblong aggregates of 1–5 nm particles. Within the aggregates and exterior to them was a second, finely crystalline phase which was enriched in ruthenium (60–70%) and depleted in molybdenum (10–20%), relative to commonly cited values of the noble phase [15].

2.2. Thermal reaction of NF_3 and the noble-metal phase

Fig. 3 presents the thermogravimetric scan of the reaction between 9 mg of the noble-metal residue and 10% NF_3/Ar; the two curves presented are the sample's mass (%) and temperature (°C) as measured by the thermocouple located on the bottom of the sample holder. When NF_3/Ar flow was introduced at 400 °C, a significant exothermic reaction resulting in an immediate 10% mass loss occurred. The exotherm, indicated by a 40 °C increase in temperature relative to the set point temperature, lasted about 3 min.

After the exothermic reaction subsided, the reaction slowed and the purge gas cooled the sample to below 400 °C. The temperature was raised slightly to see if further exothermic behavior could be observed. As none was observed, the sample temperature was raised to 500 °C and the TG instrument was held isothermal mode for ~1.5 h. A second exothermic reaction resulted with a 20 °C increase from the 500 °C set point. With approximately 20 mass% of the sample volatilized from the sample pan, the second exotherm tailed off after about 40 min., indicating continued exothermic reaction(s) over this period.

In Fig. 4, is a thermal scan of a surrogate hcp, noble-metal phase sample [26]. The data in Fig. 4 indicates that between 400 and 500 °C, the rate of mass loss was about 3% over 22 min. Assuming linear mass loss, 45% mass loss from this refractory material would have required 10 h at 500 °C. A lack of any heat evolution during the reaction completes the comparison of the surrogate material to the reaction of the high surface area, noble-metal phase in Fig. 3.

In order to compare the reactivity of the noble metal phase to its metal and oxide constituents, powders of Ru, Rh, and Pd, were reacted under the same exposure conditions as those used for the experiments presented in Figs. 3 and 4. Ruthenium metal proved to be the more reactive of the set and Fig. 5 shows the volatilization behavior of freshly reduced ruthenium metal at 400 and 500 °C in 10% NF_3. The SEM image (insert) indicates that the starting Ru metal crystallites had a uniform distribution of about 1 μm. The reaction of the metal with NF_3 at 400 °C induced a small mass increase consistent with formation of RuF_2. Note that the reaction with NF_3 in Fig. 5 shows no heat evolution at 400 or 500 °C, and while the rate of mass loss to RuF_5 was significantly faster than mass loss from the lower surface area material in Fig. 4, the 1 μm Ru metal reacted quite slowly below 400 °C, and near 500 °C, only 50% of the Ru had reacted after about 1 h.

2.3. Post-fluorination characterization of the noble metal phase

After the noble-metal phase was reacted with NF_3, the residue from the TG sample pan was collected for microscopic analyses.

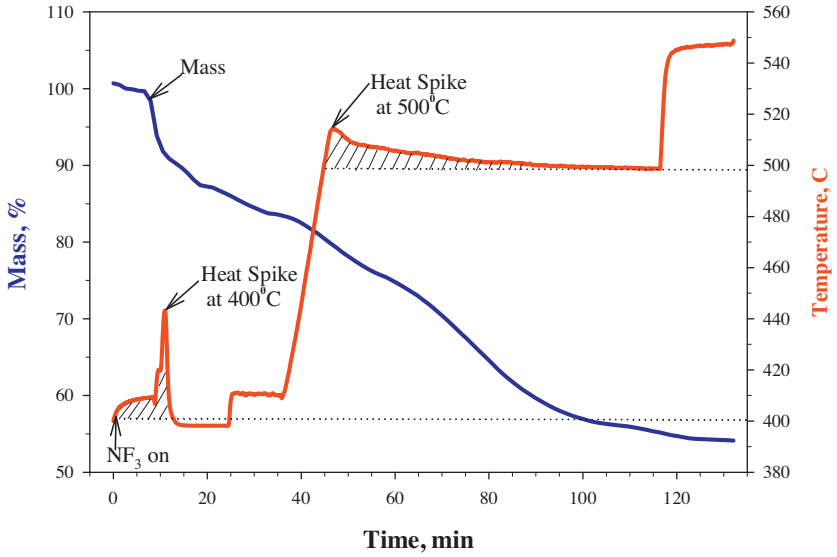

Fig. 3. TG scan of the fluorination reaction between NF_3 and the noble-metal phase. The reaction exothermicity is highlighted along the 400 and 500 °C isothermals.

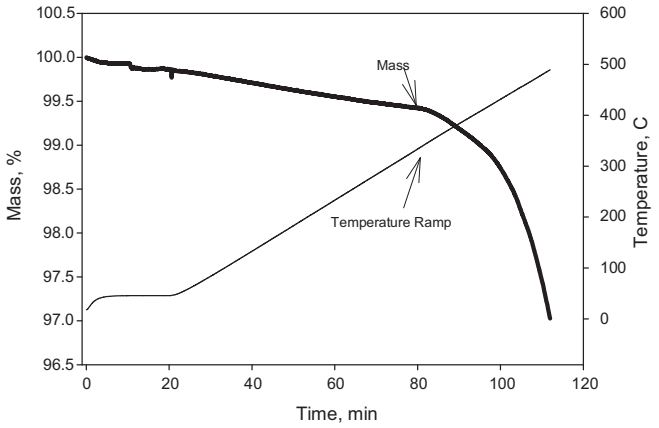

Fig. 4. TG scan of the reaction of 10% NF_3 with a surrogate noble metal epsilon phase. The furnace ramp rate was 10 °C/min up to 500 °C.

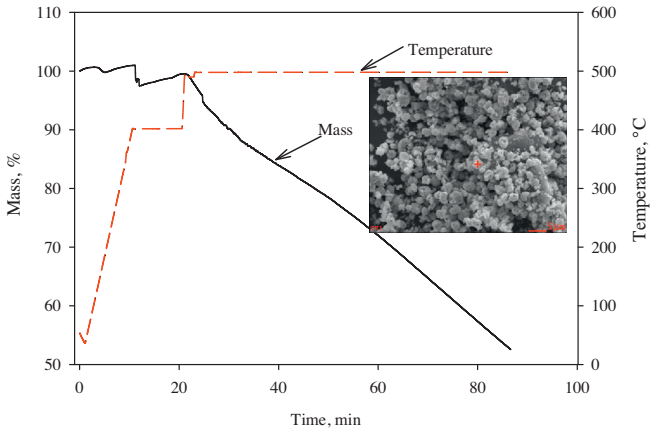

Fig. 5. TG scan of the reaction of 10% NF_3 with freshly reduced Ru metal. The insert shows the SEM image of the starting Ru metal and indicates the metal size was fairly uniform near 1 μm crystallites. Only about 50% of the metal was reacted isothermally over 1 h with very little heat production.

The SEM micrograph shown in Fig. 6 indicates the presence of two major products. One of the products appeared as small aggregates of a Pd phase (Fig. 6a), as was confirmed by its EDS spectrum. The second product was a pure Rh-F phase that appeared as crystals between 2 and 20 μm in length (Fig. 6b). Post-fluorination SEM/EDS spectra of the residue indicate that it was devoid of Mo, Tc, and Ru, for the samples analyzed; the treatment with NF_3 had extracted the Mo, Tc, and Ru from their solid solution in the noble metal

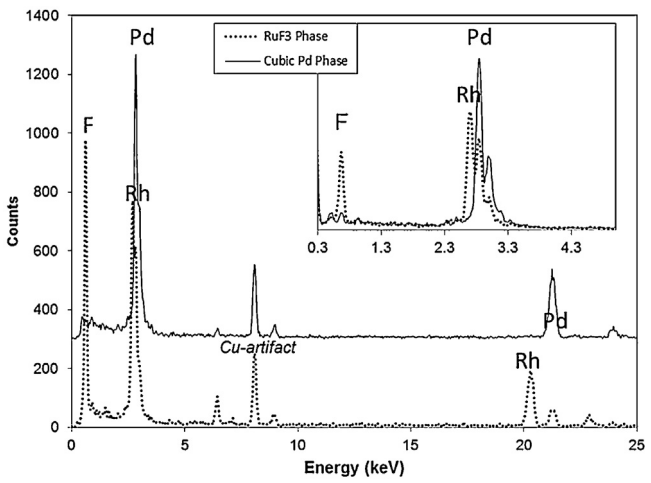

Fig. 7. X-ray energy dispersive analysis of the Pd and RhF_3 phases (the Cu-signal is due to fluorescence) and (inset) the lower energy region that reveals the fluorine in the Rh phase and clearly resolved the Rh and Pd overlap.

phase. TEM/EDS were also used to confirm that the phase was devoid of other elements to the limit of detection of these surface techniques.

The TEM/EDS data in Fig. 7 shows both the Pd and RhF_3 phase analyses. In the lower energy region, there is significant overlap between the Rh- and Pd-L lines at 2.696 and 2.838 keV, which confused their identification. The phases were more easily distinguished in the TEM by observing the higher energy K_α-lines at 20.217 and 21.180 keV for Rh and Pd, respectively.

A high resolution TEM image of the Pd product is shown in Fig. 8a. The image in Fig. 8b shows a series of lines that correspond to lattice fringes. The observation of lattice fringes demonstrates that the post-fluorination residue was a crystalline material with a very small particle size.

The electron diffraction pattern in Fig. 9 shows a ring pattern consistent with multiple small crystals. The rings in the pattern were indexed to the cubic metallic Pd phase reported in the International Center for Diffraction Data (ICDD) database [29]. Electron diffraction analysis of the phase from two different zone axes confirmed that the phase was structurally similar to Pd metal (**cubic **a** = 3.8898 Å).

The reported X-ray diffraction data from RhF_3, as well as from isostructural RuF_3 and PdF_3, indicate that many of the larger d-spacings that should be present for a hexagonal lattice were absent [30]. However, the electron diffraction pattern for the NF_3-treated residue shown in Fig. 10 shows additional reflections possibly

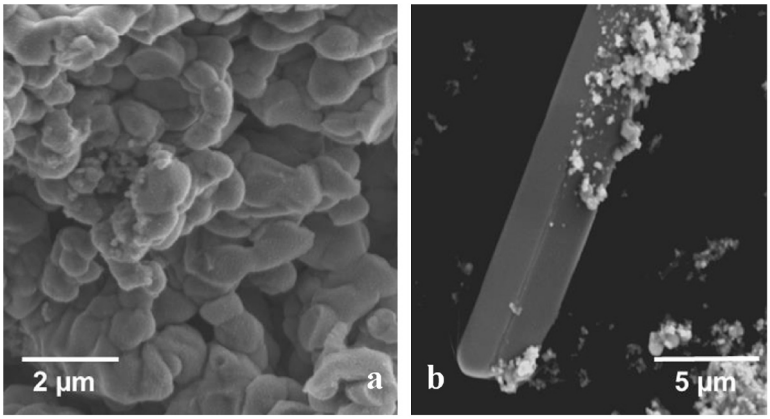

Fig. 6. Scanning electron microscopy image of (a) the Pd phase and (b) the RhF_3 phase. The Pd phase appeared as fine particulates, as small aggregates of it can be seen in (b) on the large single crystals of RhF_3.

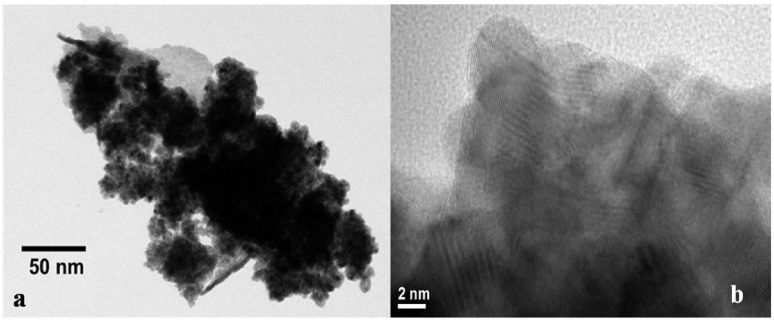

Fig. 8. (a) Medium magnification image of the Pd and Rh aggregate phases. The Rh phase occurred as well-defined elongated crystals whereas the Pd phase was present as nano-crystalline agglomerates. (b) High magnification image of the Pd phase showing the lattice fringes.

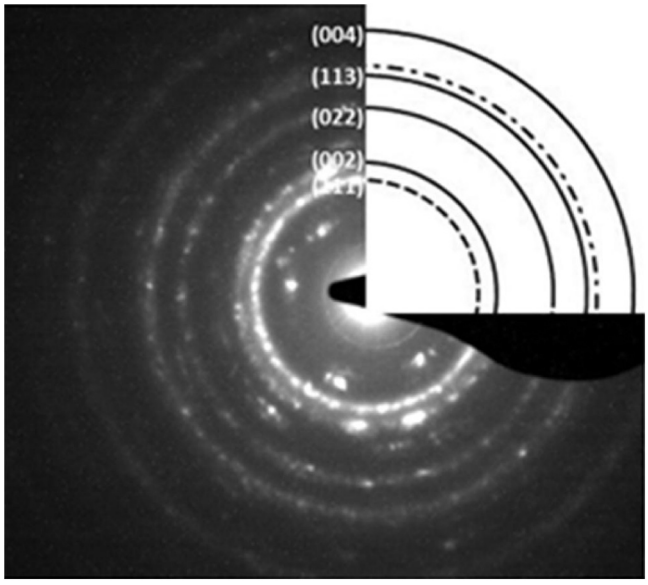

Fig. 9. Ring electron diffraction pattern of the palladium metal indicating a nano-particulate agglomerate phase. Simulation of the ring pattern is also shown with the *h k l* reflections.

owing to compositional variations compared to the pure phases reported in the literature.

The structure determined agrees well with a hexagonal lattice with **a** ~ 4.3 Å and **c** ~ 6.8 Å. A computer simulation using CrystalMaker™ software shows an excellent match between experiment and model for both the Pd and RhF_3 phases. There was no indication that the residual product contained the orthorhombic RhF_4 phase.

Pure Pd metal powder was reacted with 10% NF_3/Ar at 400 and 500 °C to understand the speciation that might arise from the noble-metal phase. The reacted powder was dark brown at 400 °C and red brown at 500 °C. The neat Pd treated at 400 °C was inert to fluorination by NF_3, but treatment at 500 °C produced a mixture of PdF_2 and PdF_3 as confirmed by their XRD powder patterns [31,32]. X-ray diffraction data acquired from the fluorinated Pd samples at 400 °C agreed well with the metal cubic phase as is described by the literature data [33] in Table 1.

3. Discussion

The metal and oxide forms of Mo, Tc, Se, and Te, react with NF_3 at temperatures between 300 and 400 °C to form volatile fluorides or oxyfluorides (see Table S1 in the Supplementary Data Section). SeO_2 volatilizes in the presence of NF_3 circa 300 °C or boils at 315 °C, so that Se may volatilize as the fluoride or oxide near 400 °C. Rh, Pu, Am, Eu, Ag, Cs, as their oxides, react with NF_3 to form their non-volatile fluorides, below 450 °C [7,8]. The volatility separation of Mo, Tc, and lower concentrations of Te and Se from the residue was thus initiated early in the thermal treatment with NF_3. The first exotherm near 400 °C in Fig. 3, is consistent with depletion of ~20% Mo, and lesser concentrations of Tc, Te, and Se, from the high surface area residue. The mass loss due to volatilization was accompanied by minor mass gain due to exothermic formation of the nonvolatile fluorinated products in the sample. The rapid temperature increase at 400 °C indicates a high velocity rate of reaction. The slow-down in heat production after 3 min does not mean the reaction was over, as is evidenced by the continued mass loss, rather that the majority components were sufficiently depleted such that self-heating was reduced to near the set point temperature.

The second exotherm near 500 °C in Fig. 3 indicates the onset of ruthenium volatility from the noble metal phase. The self-heating

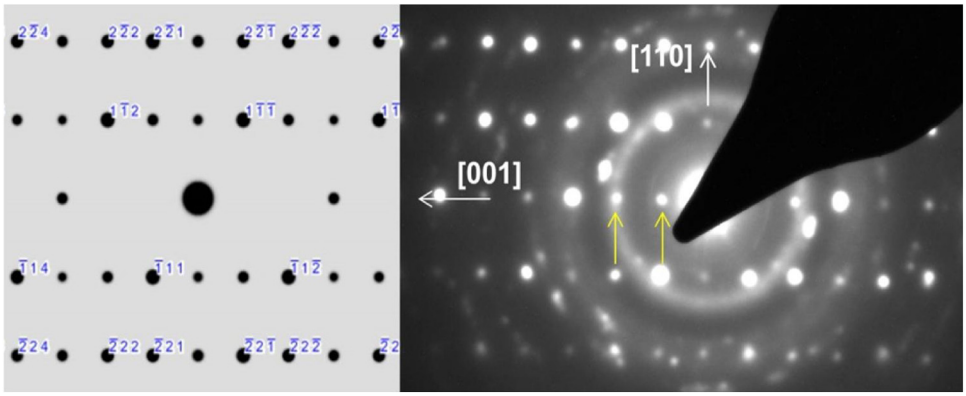

Fig. 10. Electron diffraction analysis of a single RhF_3 crystal taken along the B[0 1 0] zone axis. A faint series of reflections from the Pd phase is also visible.

Table 1
Electron diffraction data from the Pd and Rh fluoride phases.

Pd phase		Rh fluoride phase	
Measured d/Å	lit/Å[a]	Measured d/Å	lit/Å[b]
2.260	2.246	6.764	–
2.003	1.9450	4.287	4.2262
–	–	3.726	–
1.722	–	3.501	3.5909
1.403	1.3760	2.842	2.6515
1.190	1.1730	–	2.4400
–	1.1232	2.235	2.2970
0.998,1.088	0.9723	2.111, 2.136	2.1131
–	–	2.066	2.01818
0.881	0.8924	1.866, 1.838	1.98334
0.809	–		1.791

[a] Ref. [32].
[b] Ref. [31].

in the remaining ~6 mg of sample lasted for nearly 90 min. The self-heating in this small sample size again represents a substantial rate enhancement for the fluorination reaction relative to that for pure Mo, Rh, Ru, and Pd using identical exposure conditions. In fact, work in our laboratories investigating reactions of metals and metal oxides across the periodic table with NF_3 has not produced similar heat evolution data except for the fluorination of uranium and plutonium metal foils, whose reactions were hypothesized to be autocatalytic in nature [34].

One component of the pre-fluorination noble phase as highlighted in Fig. 2, was finely crystalline, enriched in ruthenium, and sharply depleted in Mo, Tc, Pd, and Rh. We speculate that this Ru component in particular might be responsible for the high initial heat production at 500 °C. The self-heating from the hottest point at 500 °C would then arise from the remaining Ru in a Ru–Rh–Pd mixed-metal phase, and would indicate either the residual ruthenium was more resistant to fluorination or that some other exothermic event, e.g., Rh fluorination, lingered after the initial portion of the ruthenium had been volatilized. Evidence for an intact Rh–Pd–Ru phase is provided by fluorination of neat Pd metal, which resulted in formation of PdF_2 and PdF_3 near 500 °C; phases not seen in the NF_3 treatment of the noble metal phase.

It is claimed that large scale volatility processing, using F_2 gas, of commercial used fuel would release the total inventory of the transition metals from the fuel [5]. In the current study, the volatile fluorides of Mo, Tc, and Ru were efficiently depleted from the noble metal phase between 400 and 550 °C ostensibly because of its large surface area. Based on the ~40 °C temperature rise observed for the initial 9 mg sample under the non-adiabatic conditions of the TG experiment in Fig. 3, it can be surmised that if a larger portion of the noble-metal phase were thermally reacted with NF_3, or a more potent reagent such as F_2, at 600 °C and under a more adiabatic condition, these and the remaining components: Ru, Rh, and Pd, would be fluorinated in a compressed time and produce a greater temperature excursion. While high heat loads are expected for fluoride volatility processing of the uranium alone in used nuclear fuel, a high surface area metallic phase may require additional constraints on processing temperatures.

Fig. 5 shows that the reaction of 10% NF_3 with freshly reduced 1 μm Ru metal approached only 50% mass loss after about 1 h at 500 °C. The slow reaction rate was accompanied by quite low heat production, in contrast to that described for the reaction of the high surface area noble phase. The lack of self-heating in the 1 μm Ru metal samples, and in the surrogate noble-metal phase is consistent with the noble character of these materials, but additionally with kinetics associated with, and retarded by, diffusion limited behavior(s) [35].

Work in our laboratory has shown the 1–5 nm particle size and morphology exists in LWR and BWR used nuclear fuels with different fuel burnups[1]. The observation of the fine-grained nature of the metal phase contrasts to most early literature [10,16] descriptions, but this feature can be seen in the higher resolution micrographs of Thomas [14] and more recently Cui [15], who also examined LWR and BWR used nuclear fuels. A second phase observed in Fig. 2, which appeared to surround the nanoparticles, was a more finely grained crystalline material, enriched in ruthenium (60–70%) and depleted in molybdenum (10–20%) and the other metals, relative to commonly cited values of the noble-metal phase [15]. The presence of the Ru-enriched phase may provide evidence that the phase is deposited throughout the fuel in this form, rather than as segregated from the noble-metal phase by radiation damage or other mechanisms. The phase has not been widely described in the literature but it is represented in the ruthenium apex of Kleykamp's pseudo-ternary phase diagram [10].

Uniform samples of such fine-grained particles are out of the ordinary from a fundamental chemical standpoint. Special preparatory techniques are generally required to produce similar particle sizes and narrow particle size distribution. In addition to these features, the pure phase nature of the major compositions [10,15] may be pertinent to the material's reactivity. It is possible that active surface sites, in particular on Ru–Pd–Rh mixed metal particles, may act to encourage surface adsorbtion of small molecules and lower activation barriers to their reaction. The reactivity toward NF_3 is consistent with laboratory simulations of accident scenarios, wherein fuel [19] and fuel simulants were strongly heated with oxidants or in oxygen directly, leading to rapid release of Ru, for instance, as an oxide, e.g., RuO_4 [20].

The TEM data coupled to literature reports confirmed the residual products of fluorination as a palladium cubic metal phase and large crystals of RhF_3. In contrast, fluorination of neat Pd metal produced a mixture of PdF_2 and PdF_3, and only small crystallites were obtained by fluorination of Rh metal. The differences between the alloyed and neat materials suggest that fluorination of the noble phase did not liberate Pd and Rh metal, rather, Tc and Mo were extracted leaving something other than pure, separated metal particulates. The variable composition of our noble phase materials certainly contained a significant fraction of the hcp phase [10], however, it is plausible that variation in phase composition, e.g., Pd cubic inclusions may not have been detected in our sampling. Alternately, we require a mechanism that would allow the metallic palladium phase to become cubic from the hcp noble parent, below 500 °C. Likewise, fluorination of Rh can produce RhF_3, RhF_4, and the volatiles: RhF_5 and RhF_6 [36,37]; nevertheless, only the lower fluoride with a unique morphology was observed. Fluorination reactions of heterogeneous solids typically produce well-formed but flat crystals because the short duration of fluorination limits crystal growth. The formation of the cubic Pd metal, the lower-valent RhF_3, as well as its large crystal size thus might involve an intact Ru–Rh–Pd alloy at 500 °C in Fig. 3. Fluorination of an Ru–Rh–Pd alloy might initially result in higher oxidation state fluorides. Historically, isolation and characterization of the higher valent fluorides: RuF_5, RuF_6 [38], PdF_4, PdF_6 [39,40], RhF_5, RhF_6 [41], proved to be difficult because of their thermal instability or their extreme reactivity. It is plausible that a fluorinated, Ru–Rh–Pd alloy would partition, on reaction with NF_3, to the higher fluorides and these products rapidly donate fluorine by their thermal decomposition to lower oxidation state Rh fluoride(s) and the cubic Pd metal. The overall mechanism would

[1] High resolution TEM analysis of 3 LWR and BWR fuels having varying burn-up, as dissolved in boiling 12M HNO_3 and also in ammonium carbonate/30% hydrogen peroxide, show the 1–5 nm particles size and variation in phase are common to each fuel and for both processing types.

then be similar to the iodide process [42] that is used for metals crystal growth.

Finally, as concerns the separation of the noble phase constituents, volatile Tc, Mo, and Ru, fluorides were recovered at their exit from the TG apparatus by passing them through a water bubbler. The palladium metal and the RhF_3 residual solids were further separated by dissolution of RhF_3 in dilute hydrofluoric acid, wherein the palladium did not dissolve.

4. Conclusions

The use of NF_3 allowed a programmed temperature desorption of the volatiles Mo, Tc, Se, and Te, from Ru in the noble metal phase. Mo, Tc, Se, and Te were volatilized near 400 °C and Ru was released near 500 °C from the nonvolatile residue. The solid residue after fluorination contained a nanocrystalline palladium metal phase and a hexagonal RhF_3 phase. Palladium metal was not observed for fluorination of neat palladium powders and we observed growth of 1–20 μm-sized acicular crystallites of RhF_3. The latter was unique to our experience with fluorination reactions of oxides and metals because crystal growth is usually inhibited by the short duration (1–2 h) required to complete fluorination reactions. Both results indicate that an intact alloy remained after volatilization of Mo and Tc from the native noble metal phase.

Evidence for high velocity rates of fluorination and excessive heat production for the fluorination of the noble-metal phase has been provided, and this enhanced chemical reactivity is surmised to be accentuated by the nanoparticulate nature of the phase. The data herein are the first to directly observe reactivity of an isolated noble-metal phase and correlate it to its high surface area or catalytic potential but these results could be important during the recovery of used nuclear fuel, during nuclear reactor accident scenarios, or for the permanent disposal of used fuel.

Fluoride volatility appears to be a rapid approach for separation and recovery of the platinum metals: Ru, Rh, and Pd, from residues of dissolved used nuclear fuel. The inability of NF_3 to fluorinate Pd and Rh from the noble metal phase does not imply that higher temperature, use of fluorine gas or a more aggressive fluorinating reagent would not do so. The rapid partitioning of the noble phase and residues of used fuel dissolution into two volatile fractions (Mo,Tc, Se, Te, and Ru) and a non-volatile fraction, adds NF_3 to the list of fluorinating reagents needed for complex separations design.

5. Experimental

5.1. Materials

The metal phase used was obtained by dissolving approximately 15 g of a high burn-up boiling water reactor (~70 MWd/kgU) fuel in 1.5 M ammonium carbonate solution with 30% hydrogen peroxide as oxidant [17]. The residue of dissolution was collected and washed with 0.5 M HNO_3, rinsed with water at room temperature, to remove residual plutonium, uranium, alkali and alkaline earth fission products to below detectable levels as confirmed by TEM.

The gases used for the thermoanalytical experiments were 99.995% purity NF_3 from Advanced Specialty Gases (Reno, NV) and 99.9995% argon from OXARC (Pasco, WA). Metal powders 99.9%, <1 μm palladium metal, 99.95%, 1 μm rhodium oxide powder, 99.9%, 74 μm ruthenium oxide were purchased from Sigma–Aldrich.

5.2. Thermogravimetric analyses

Spent fuel residues were placed in a nickel sample pan and were exposed to 10% NF_3/Ar at 200 mL/min in a Seiko 6200 series thermal gravimetric (TG) apparatus housed in a glovebox. The TG instrument, adapted and modified for radiological and fluorination studies, has been reported elsewhere [6]. Various temperature ramps were tested to understand onset temperatures for the reactions discussed.

The mass of the used fuel residue sample reported here was 9 mg. The sample was heated at 10 °C/min to 400 °C in Ar, then the 10% NF_3/Ar flow was started, and the sample was held isothermal at 400 °C for 40 min. The sample was then heated to 500 °C at 10 °C/min, held isothermal at 500 °C for 1 h, and was finally heated to 550 °C to complete the reaction, as indicated by gravimetric measurement of a constant mass.

The volatile fraction containing the chalconide fluorides and transition metal fluorides was collected from the output of the TG in water at room temperature. A small portion of the fluorinated residue remaining in the sample pan was mounted on carbon tape and carbon coated for analysis by SEM/EDS. The TEM samples of the fluorinated residue were prepared as described above.

Approximately 20 mg of Pd metal, RuO_2, Rh_2O_3, SeO_2, and TeO_2 powders, were reacted with 10% NF_3 in argon to determine if their volatile fluorides would form and the temperature conditions required for their complete volatilization (See Table S1 in the Supplementary Data Section). RuO_2 (74 μm) and Rh_2O_3 (100 μm) were reduced in the TG with 5% hydrogen at a flow rate of 200 mL/min to their respective metals near 700 °C. The reductions required about 1 h to achieve theoretical mass loss. The initial RuO_2 powder had a particle size of 74 μm and that was altered by its reaction with hydrogen to about 1 μm particles. The crystalline particles of the Ru metal were fairly uniform, around 1-μm. The Rh metal product evidenced a similar size reduction from its reduction in hydrogen. Each metal was immediately reacted with 10% NF_3 to support results of the thermal analysis of the noble metal phase.

The noble-metal phase surrogates were prepared from the five metals: Mo, Ru, Rh, Pd, and Re (surrogate for Tc), using advanced thermal methods [26]. The material was difficult to break or grind to smaller size [26] for its TG analysis. Consequently, small (50–70 mg) pieces obtained by cutting the alloy with metal snips were used for thermoanalytical studies of its reaction with 10% NF_3/Ar. Conditions were the same as used for the actual noble phase material.

5.3. Microscopy

The morphology and elemental content of the initial and post fluorinated noble phase was characterized using SEM coupled with EDS and TEM. For SEM analyses, a few fragments of the residue were placed on a clean glass slide. Larger agglomerates were crushed by laying another glass slide on top and applying pressure with a tungsten scribe. A pipette containing a small amount of methanol was used to extract a few particles. These were then deposited on a sticky carbon tape, coated with conductive carbon and analyzed with an FEI (Hillsboro, OR, USA) Quanta250 field emission gun scanning electron microscope equipped with an EDS (EDAX Inc., Mahwah, NJ) compositional analysis system running GENESIS analysis software. Microscopic images were obtained under secondary and backscattered electron imaging conditions, single point, line scans, and X-rays maps were collected.

For TEM analyses, a small number of particles were isolated, and were picked up in 2 mL ethanol, then diluted by addition of a few drops of the first suspension into 2 mL of fresh ethanol. The diluted suspension was agitated by sonication. A drop of the solution was added to a copper TEM grid and allowed to dry. The samples were examined on a FEI Tecnai T30 transmission electron microscope with a LaB6 gun operated at 300 keV. The microscope was equipped with a Gatan (Gatan Inc., Pleasanton, CA) ORIUS™ digital camera and an EMiSpec EDS system. The electron diffraction

camera lengths were checked against a MAG*I*CAL silicon standard, as were the length scales.

Diffraction patterns and electron micrographs were analyzed with Gatan DigitalMicrograph™ 1.83.842 and custom scripts by Mitchell [43]. Crystal models and simulated diffraction pattern were generated using CrystalMaker® 2.2, a crystal and molecular structures program for Mac and Windows, and SingleCrystal®2.0.1, an electron diffraction simulation program distributed by CrystalMaker Software Ltd., Oxford, England.

5.4. XRD

X-ray powder patterns were acquired using a Rigaku Ultima IV X-ray diffractometer to aid in determination of the stoichiometry of the fluorinated products. Milligram quantities of the samples were placed in 0.7-mm capillary (Charles Supper Co, Natick, MA) tubes and epoxied closed. The capillary tubes were encapsulated in polyester heat shrink tubing (Salem, NH). Data was acquired between 2 and 60 degrees 2-theta on a capillary attachment with spinner capability. Samples were rotated at 40 RPM.

Acknowledgements

The work described in this article was performed by Pacific Northwest National Laboratory (PNNL), which is operated by Battelle for the United States Department of Energy (DOE) under Contract DE-AC05-76RL01830. The DOE-Nuclear Energy's Fuel Cycle Research and Development Program and PNNL's Sustained Nuclear Power Initiative funded our efforts. We would like to thank J. Crum, D. Strachan, A. Rohatgi, and M. Zumhoff for providing us with a sample of their surrogate epsilon metal phase and to A. Kozelisky for her thermoanalysis of the product.

Appendix A. Supplementary data

Supplementary data associated with this article can be found, in the online version, at http://dx.doi.org/10.1016/j.jfluchem.2014.02.010.

References

[1] A.A. Jonke, Atom. Energy Rev. (Austria) 3 (1965) 3–60.
[2] N.M. Levitz, L.J. Anastasia, E.L. Carls, A.A. Chilenskas, J.A.E. Graae, A.A. Jonke, R.A. Kessie, R.P. Larsen, W.J. Mecham, D. Ramaswami, M.J. Steindler, G.J. Vogel, Argonne National Laboratory (1969).
[3] V.V. Shatalov, M.B. Seregin, V.F. Kharin, L.A. Ponomarev, Atom. Energy 90 (2001) 224–234.
[4] A.A. Jonke, N.M. Levitz, M.J. Steindler, Nucl. Met. Met. Soc. AIME 15 (1969) 231–240, From Symposium on Reprocessing of Nuclear Fuels, See CONF-690801, (1969).
[5] J. Uhlíř, M. Mareček, J. Fluorine Chem. 130 (2009) 89–93.
[6] B.K. McNamara, R.D. Scheele, A.E. Kozelisky, M. Edwards, J. Nucl. Mater. 394 (2009) 166–173.
[7] R.D. Scheele, B.K. McNamara, A.M. Casella, A.E. Kozelisky, J. Nucl. Mater. 424 (2012) 224–236.
[8] R.D. Scheele, B.K. McNamara, A.M. Casella, A.E. Kozelisky, D. Neiner, J. Fluorine Chem. 146 (2013) 86–97.
[9] H. Kleykamp, J.O. Paschoal, R. Pejsa, F. Thümmler, J. Nucl. Mater. 130 (1985) 426–433.
[10] H. Kleykamp, J. Nucl. Mater. 131 (1985) 221–246.
[11] J.L. Bramman, R.M. Sharpe, D. Thom, G. Yates, J. Nucl. Mater. 25 (1968) 201–215.
[12] H. Kleykamp, J. Nucl. Mater. 171 (1990) 181–188.
[13] M.H. Kaye, B.J. Lewis, W.T. Thompson, J. Nucl. Mater. 366 (2007) 8–27.
[14] L.E. Thomas, R.E. Einziger, R.E. Woodley, J. Nucl. Mater. 166 (1989) 243–251.
[15] D. Cui, V.V. Rondinella, J.A. Fortner, A.J. Kropf, L. Eriksson, D.J. Wronkiewicz, K. Spahiu, J. Nucl. Mater. 420 (2012) 328–333.
[16] RardF J.A., AndereggF G., WannerF H., RandF M.H., Chemical thermodynamics of technetium, Elesvier Sciences B.V., Amsterdam, the Netherlands, 1999.
[17] C.Z. Soderquist, A.M. Johnsen, B.K. McNamara, B.D. Hanson, J.W. Chenault, K.J. Carson, S.M. Peper, Indust. Eng. Chem. Res. 50 (2011) 1813–1818.
[18] C.Z. Soderquist, B.M. Hanson, J. Nucl. Mater. 396 (2010) 159–162.
[19] International Atomic Energy Agency, Control of Semivolatile Radionuclides in Gaseous Effluents at Nuclear Facilities, 1982 Technical Reports Series No. 220.
[20] C. Mun, L. Cantrel, C. Madic, Nucl. Technol. 156 (2006) 332–346.
[21] D. Cui, Progr. Chem. 23 (2011) 1411–1428.
[22] M.E. Broczkowski, J.J. Noël, D.W. Shoesmith, J. Nucl. Mater. 346 (2005) 16–23.
[23] Z. Kolarik, E.V. Renard, Platinum Met. Rev. 49 (2005) 79–90.
[24] Z. Kolarik, E.V. Renard, Platinum Met. Rev. 47 (2003) 123–131.
[25] Z. Kolarik, Platinum Met. Rev. 47 (2003) 74–87.
[26] J.V. Crum, D. Strachan, A. Rohatgi, M. Zumhoff, J. Nucl. Mater. 441 (2013) 103–112.
[27] T. Adachi, M. Ohnuki, N. Yoshida, T. Sonobe, W. Kawamura, H. Takeishi, K. Gunji, T. Kimura, T. Suzuki, Y. Nakahara, T. Muromura, Y. Kobayashi, H. Okashita, T. Yamamoto, J. Nucl. Mater. 174 (1990) 60.
[28] S. Vaidyanathan, R.D. Reager, R.W. Warner, High burnup BWR fuel pellet performance, in: Proc. 1997 Intl Topical Meeting on LWR Fuel Performance, 1997, 471–477.
[29] ICCD, Release 2013, International Center for Diffraction Data, Newton, PA, 2013.
[30] M.A. Hepworth, K.H. Jack, D. Peacock, G.J. Westland, Acta Crystallogr. 10 (1957) 63–69.
[31] F. Ebert, Gruppe des Periodischen Syst. 196 (1931) 395–402.
[32] N. Bartlett, R. Maitland, Acta Crystallogr. 11 (1958) 747–748.
[33] H.E. Swanson, E. Tatge, Standard X-ray diffraction powder patterns, U. S. Circular No. 539, National Bureau of Standards, Washington, D.C., 1953.
[34] B.K. McNamara, R.D. Scheele, A.M. Casella, A.E. Kozelisky, D. Neiner, Fluorination of uranium metal to UF_3 and UF_4 by nitrogen trifluoride: evidence for elusive UF_2, in: MRS Proceedings, Basic Actinide Science and Materials for Nuclear Applications, 2010, p. 1264.
[35] A.M. Casella, R.D. Scheele, B.K. McNamara, Trans. Am. Nucl. Soc. 105 (2011) 215–217.
[36] W.P. Griffith, The Chemistry of the Rarer Platinum Metals (Os, Ru, Ir, and Rh), Interscience, New York, 1967.
[37] A.V. Dzhalavyan, E.G. Rakov, A.S. Dudin, Russ. Chem. Rev. 52 (1983) 1676–1697.
[38] H.H. Claassen, H. Selig, J.G. Malm, C.I. Chernick, B. Weinstock, J. Am. Chem. Soc. 83 (1961) 2390–2391.
[39] P.R. Rao, A. Tressaud, A.N. Bartlett, J. Inorg. Nucl. Chem. 28 (1976) 23–28.
[40] G. Aullon, S. Alvarez, Inorg. Chem. 46 (2007) 2700–2703.
[41] W.M. Schwarz, E.M. Kowsower, I. Shain, J. Am. Chem. Soc. 84 (1961) 3165–3166.
[42] A.E. Van Arkel, J.H. de Boer, Zeitschrift für Anorganische Chem. 48 (1925) 345–350.
[43] D.R.G. Mitchell, Microsc. Res. Technol. 71 (2008) 588–593.